

Prediction of isolated and thermal point defects in B2 aluminium-based crystalline compounds of transition metals AlTM (TM = Ru, Ir, Os and Rh)

A. Kerboub^a, H. Louafi^b, B. Zaidi^{b,*}, E. Belbacha^a

^aLaboratory of physical chemical study of materials (LEPCM), Department of physics, Faculty of matter sciences, University of Batna 1, Algeria

^bDepartment of physics, Faculty of matter sciences, University of Batna 1, Algeria

The present paper reports the studies on Aluminum-based crystalline compounds AlTM (TM =Ru, Ir, Os and Rh).The random pseudobinary ($A_{1-x}B_xC$) compounds with compositions $x = 0.25$ and 0.5 have been investigated using Special Quasirandom Structures (SQS) approach. First principle calculations have been performed to investigate types of defect present in non-stoichiometric B2 AlTMphase. The results indicate that the Al-antisite defect and TM-antisite defect are the main defects present along Al-rich side and TM-rich side respectively. Additionally, at finite temperature along the Al-rich region, Al vacancies and along TM-rich side, TM vacancies which are the constituents of Schottky defect are the main thermal defects in B2 AlTM respectively.

(Received January 31, 2025; Accepted April 22, 2025)

Keywords: Point defects, Special quasirandom structures (SQS), Wagner Schottky model

1. Introduction

Aluminium-based crystalline compounds of transition metals are the most important class among the high-performance structural materials, excellent strength at increased temperatures, resistance to oxidation and corrosion, relatively low density, and a high melting point are some of their attractive characteristics [1]. B2-type intermetallic with transition metals and Aluminum Among these alloys, AlTMs represents a unique class of materials that exhibit a wide range of fascinating physical phenomena [2].

The current paper is concerned with four Aluminum-based crystalline compounds of transition metals AlTM (TM =Ru,Ir,Os and Rh). The AlIr and AlRu alloys have an unusual combination of properties due to the good thermodynamic stability at high-temperature environment, these metalsalso exhibit strong resistance to oxidation and corrosion, coupled with an exceptionally high melting point of approximately 2323 K. [3-5]. The alloys AlOs and AlRh share a B2 crystal structure similar to AlCo [6]. They are recognized for their potential as structural materials suitable for diverse operational environments due to the low compressibility, high bulk modulus and high catalytic potential for a wide range of chemical reactions [7]. They are employed in high-friction applications, including electrical contacts, instrument pivots, and fountain pen tips etc[8].

Point defects constitute one of the key factors to determine properties and characteristics in a crystalline material where much of solid-state technology is associated with point defects [9], and indeed this topic is central to many of the researches in materials science [9,10]. Within the past few years, many works have concentrated their attention to the studies of defect structures in B2 phase for several intermetallic compounds [11-13].

Characterization of the defects in solids can be performed by employing either experimental measurements [14] or using first-principles calculations [15]. First-principles calculations are considered as a powerful approach that complements experiments and can be used as a predictive tool for the identification of defects in materials [11]. The first principle calculations can be performed using various methods such as the Special Quasirandom Structure

*Corresponding author: beddiaf.zaidi@univ-batna.dz

<https://doi.org/10.15251/JOR.2025.212.263>

(SQS) [11,13] and the super cell approach [16, 17]. These methods are simple and applicable to the vast variety of crystals as only atomic numbers and crystal structure information are required for the application of these methods [13].

The main results of this study are the prediction of the specific types of isolated point defects found in B2 AITM compounds; by determination of the enthalpy of formation as a function of composition using first principle calculation employing SQS approach. Al-antisite defect was found to be the predominant defect in Al-rich side, meanwhile the TM-antisite is the stable defect in (TM)-rich side. For the AlRu and AlIr, we have a good agreement between our calculations and the theoretical investigations by [18] and [19] respectively, moreover, close agreement with experimental findings was observed in [20,]. In the case of AlOs and AlRh once more our calculations demonstrate strong concordance with both theoretical predictions and experimental observations, as referenced in [20, 22]. At finite temperature and using Wagner-Schottky model, we found that the predominant thermal defects in the four alloys studied are of Schottky-type.

2. Computational methodology

2.1. Special quasirandom structure (SQS)

The concept of the Special Quasirandom Structure (SQS), introduced by Zunger et al. [23], provides the most precise periodic super cell approximation to the actual disordered state for a specific number of atoms per supercell. Utilizing a special quasirandom structure (SQS) offers an efficient method for approximating random alloys. A wide range of physical properties of materials have been successfully estimated by combining SQS calculations with density functional theory (DFT). This combination is also widely employed in the study of point defects in materials. The SQS designs small-unit-cell periodic structures containing typically 8 to 32 atoms per unit cell. These structures are crafted to closely replicate the key local pair and multi-site correlation functions found in random substitution alloys [24,25]. Recently, this method has also been applied to both FCC and BCC transition metal systems, demonstrating its effectiveness [26]. The SQS approach has also been developed to investigate Formation enthalpy [27], Lattice parameters [28], Elastic [29], Magnetic [30], Electronic [31], Paramagnetic [32] and Piezoelectric properties [33].

In our study, SQS-4 ($A_{0.5}B_{0.5}C$) and SQS-16 ($A_{0.75}B_{0.25}C$) structures proposed by Jiang et al. [11] were utilized. From these structures, Al antisite ($TM_{0.75}Al_{0.25}Al$), Al vacancy ($Al_{0.75}Va_{0.25}TM$), TM antisite ($Al_{0.75}TM_{0.25}TM$) and TM vacancy ($TM_{0.75}Va_{0.25}Al$) in the SQS-16 structure, and Al antisite ($TM_{0.5}Al_{0.5}Al$), Al vacancy ($Al_{0.5}Va_{0.5}TM$), TM antisite ($Al_{0.5}TM_{0.5}TM$) and TM vacancy ($TM_{0.5}Va_{0.5}Al$) in the SQS-4 structure were generated. The enthalpies of formation for isolated point defects, as depicted in **Fig. 1** and **Fig. 2** with four branches, were determined by fitting the enthalpies of formation calculated at various concentrations. This fitting was accomplished using a quadratic function of the alloy composition [11].

2.2. Defects at different temperatures

In the study of point defects in B2 AITM alloys (where TM = Ru, Ir, Os, and Rh) were investigated. It is assumed that the defect concentration is sufficiently low to apply the Wagner-Schottky model. According to this model, defects are treated as a gas of non-interacting point defects occupying well-defined sublattices [34, 35]. This approach enables the calculation of point defect concentrations based on variations in alloy composition and temperature. A canonical ensemble with a fixed number of Al and TM (Ru, Ir, Os, Rh) atoms has been employed. When vacancies are present and the total number of lattice sites is variable, it is more practical to use atomic concentration rather than site fraction to describe defect concentration [36-38]. This method provides a simpler representation and facilitates the analysis of defect concentrations within the alloy system.

The equilibrium concentrations of point defects can be determined by minimizing the Gibbs free energy of the system. This minimization process, subject to mass balance constraints, results in a set of nonlinear equations, as described in reference [39]. These equations govern the

equilibrium point defects concentrations in the system and provide valuable insights into the thermodynamic behavior of the material.

2.3. First-principles calculations details

DFT calculations were carried out using the (PAW) pseudopotential method [40,41], applying the (PBE) generalized gradient approximation for the exchange-correlation functional [42]. These calculations were implemented within the Vienna ab-initio simulation package (VASP). We employed a plane-wave basis energy cutoff of 500 eV, and the k-point grids were generated using VASP's fully automatic meshing scheme [43], which produces centered Monkhorst-Pack grids [44]. The Brillouin zone integration was conducted using the Methfessel-Paxton technique with a smearing parameter of 0.1 eV. All computations were conducted utilizing the "Accurate" setting within VASP. Structural relaxation was achieved by allowing all degrees of freedom, including cell shape, atom positions, and volume, to relax using a preconditioned conjugate gradient (CG) method with default VASP convergence criteria. The relaxed structures obtained were analyzed using the SGROUP program [45] to ensure they retained their initial space group symmetry.

3. Results and discussion

3.1. Formation enthalpies

The SQS method calculates the formation enthalpy of AITM compounds for four types of point defects: Al antisite, TM antisite, Al vacancy, and TM vacancy. These enthalpies are individually plotted against the Al composition.

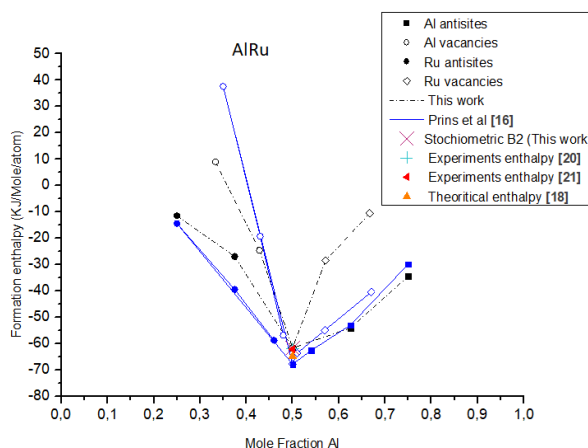


Fig.1. Formation enthalpy of AlRu: comparison of our SQS results with supercell results, experimental and theoretical enthalpies.

The formation enthalpy of B2 AlRu simulated using the SQS approach is depicted Fig.1. These results are compared with formation energies obtained from both the SQS approach and the supercell method, alongside experimental and theoretical enthalpies. The graph demonstrates a close agreement between our results and experimental findings [20], as well as theoretical calculations [18], with differences not exceeding 2 kJ/mol (≈ 0.021 eV/atom) for stoichiometric AlRu. Similar discrepancies have been reported in prior studies on metal oxides and organic systems, where differences exceeding 2.5 kJ/mol arose from varying computational parameters, including k-point density and basis set selection [21, 36, 37]. Furthermore, the graph reveals that in the Al-rich region of AlRu, Al antisite atoms exhibit greater stability compared to Ru vacancies, establishing them as the most energetically favorable type of point defect. Conversely, in the Ru-

rich region, Ruantisites exhibit greater stability than Al vacancies. Consequently, Al antisites and Ruantisites emerge as the most stable point defects in AlRu. Overall, Fig.1 demonstrates that our calculations of formation enthalpies obtained using the SQS approach align well with those obtained through the 16, 32 and 54-atom supercell methods [16,46]. This agreement has also been supported by other studies [47], indicating a consensus on the order of formation energies for the most stable point defects.

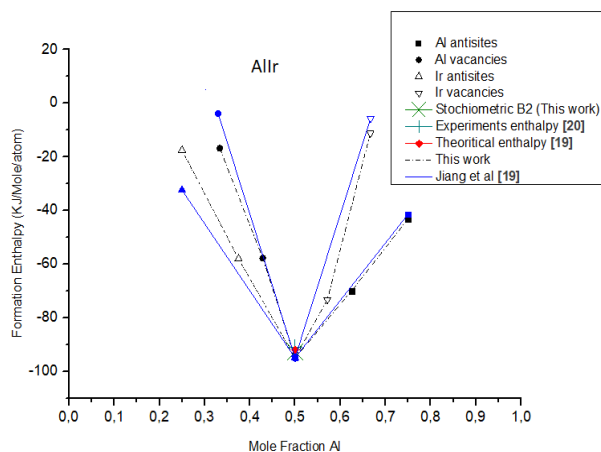


Fig.2. Formation enthalpy of AlIr: comparison of our SQS data with results of other SQS, experimental and theoretical enthalpies.

Fig.2 presents the formation enthalpy of B2 AlIr, simulated using the SQS approach, and alongside energies of formation obtained through both the SQS approach and the supercell method [19]. Additionally, the graph compares the formation enthalpy of stoichiometric AlIr with experimental data [20] and theoretical work [19].

Fig.2 demonstrates a good agreement between our SQS calculations and both SQS and supercell results [19]. Although there are minor variations in the formation energies among the four types of defects, our SQS results, combined with those of [19], confirm that in the Al-rich region of AlIr, Al antisite atoms exhibit greater stability than Ir vacancies, making them the most favorable point defects in this context. Conversely, in the Ir-rich region, Irantisites are found to be more stable than Al vacancies, suggesting that both Irantisites and Al antisites are the most energetically stable types of point defects in AlIr compounds.

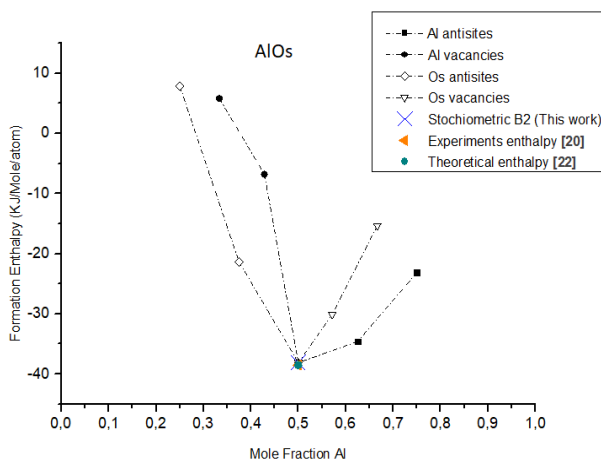


Fig.3. Formation enthalpy of AlOs :comparison of SQS results with experimental and theoretical enthalpies.

Fig.3 displays the formation enthalpy of B2 AIOs, simulated using the SQS approach. It also compares the formation enthalpy of stoichiometric AIOs with experimental data from [20] and theoretical work from [22], revealing a discrepancy of 1 kJ/mol attributable to differences in calculation conditions.

The graph showcases good agreement between our SQS results and those of [22], supporting the conclusion that in the Al-rich region of AIOs, Al antisite atoms are more stable than Os vacancies, making them the most stable point defects in this context. Conversely, in the Os-rich region, Osantisites are more stable than Al vacancies, suggesting that Al antisites and Osantisites are the most energetically stable point defects in AIOs.

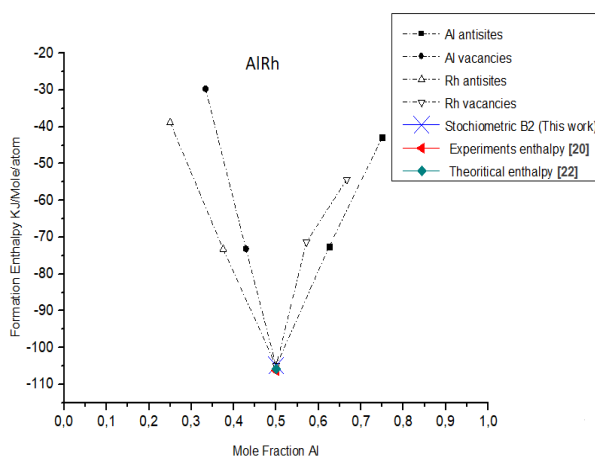


Fig.4. Formation enthalpy of AlRh :comparison of SQS data with experimental and theoretical enthalpies.

Fig.4 demonstrates a good agreement in the formation enthalpy between our results and both the experimental data from [20] and theoretical results from [22], with differences not exceeding 1 kJ/mol for stoichiometric AlRh. These variations can be attributed to differences in calculation conditions. In the Al-rich phase of AlRh, the data suggests that Al antisite atoms are more stable than Rh vacancies, indicating a preference for Al antisite atoms as the energetically favored point defects. Conversely, in the Rh-rich region, Rh antisites show greater stability compared to Al vacancies. Therefore, Al antisites and Rh antisites are identified as the most stable point defects in AlRh.

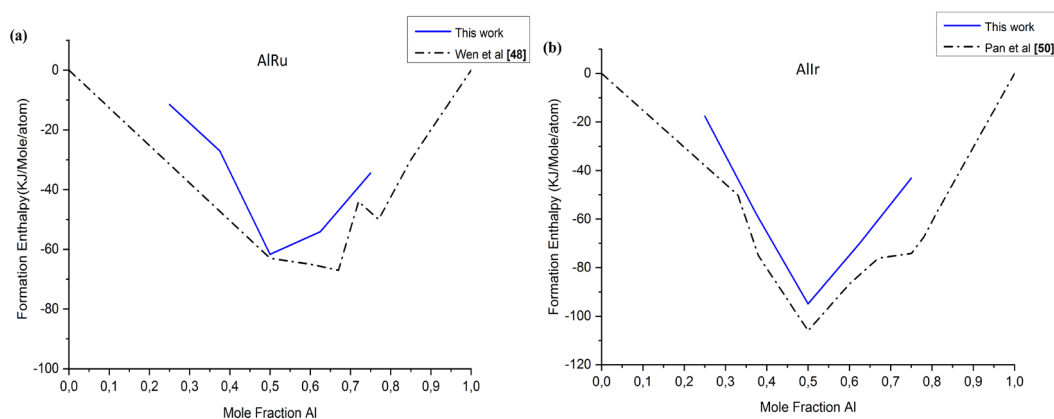


Fig.5. Formation Enthalpies of AlRu and AlIr diagram as at $T=0K$ compared with CALPHAD calculations results: (a) AlRu and (b) AlIr.

Fig.5 displays the formation enthalpies of the AlRu and AlIr systems, incorporating point defects, obtained using the SQS approach. Our findings are compared with enthalpies reported by Wen et al [48] for AlRu and Pan et al [49] for AlIr, using the CALPHAD method. For the stoichiometric AlRu and AlIr, the comparison demonstrates strong agreement between our DFT-SQS results and those derived from the CALPHAD approach. The similarity in the shape of curves confirms the validity of our results. The difference between the SQS results and the enthalpies calculated using the CALPHAD method is probably attributable to the presence of vacancies or antisites, which are not typically considered in the CALPHAD method. The inclusion of point defects in the AlRu and AlIr compounds leads to an increase in the formation enthalpies values for these alloys, but they still remain close to the results obtained from CALPHAD.

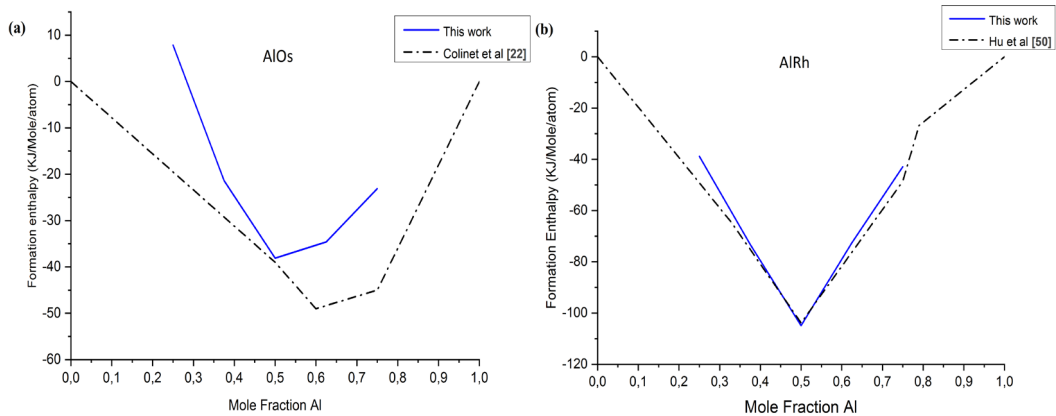


Fig.6. Formation Enthalpies of AlOs and AlRh diagram at $T = 0K$ compared with CALPHAD calculations results: (a) AlOs and (b) AlRh.

In Fig.6, the formation enthalpies of the AlOs and AlRh systems, including point defects, obtained using the SQS approach, are plotted. These results are compared with enthalpies obtained by Colinet et al. [22] for AlOs and Hu et al. [50] for AlRh using the CALPHAD method. Our results agree with those obtained using the CALPHAD approach. The variation between the SQS results and the enthalpies calculated using the CALPHAD method is likely caused by the occurrence of vacancies or antisites, which are not accounted for in the CALPHAD. However, the inclusion of point defects in the AlOs and AlRh compounds leads to an increase in the formation enthalpies values for these alloys, but they still remain close to the results obtained from CALPHAD. A good agreement between our DFT-SQS results and those derived from the CALPHAD approach for the stoichiometric AlOs and AlRh. The similarity in the shape of curves confirms the validity of our results.

3.2. Lattice parameter

Fig.7, 8, 9 and 10 illustrate the lattice parameter of B2 AITM (TM = Ru, Ir, Os, and Rh) calculated using the SQS approach, compared with available experimental and theoretical data. These figures also show the lattice parameter calculated for AITM compounds containing the two most stable types of point defects: Al antisite and TM antisite. Each defect type is plotted separately, resulting in two distinct branches.

According to our results, AITM (TM = Ru, Ir, Os, and Rh) exhibit the same types of point defects, with Al antisites dominating the Al-rich region and TM antisites dominating the TM-rich region, as shown in Figures 7 to 10, respectively. Consequently, it is evident that as the concentration of antisite defects increases, the lattice parameter also increases. This observation aligns with the findings of [16, 46], which investigated the volume evaluation of AlRu using the supercell approach with different sizes.

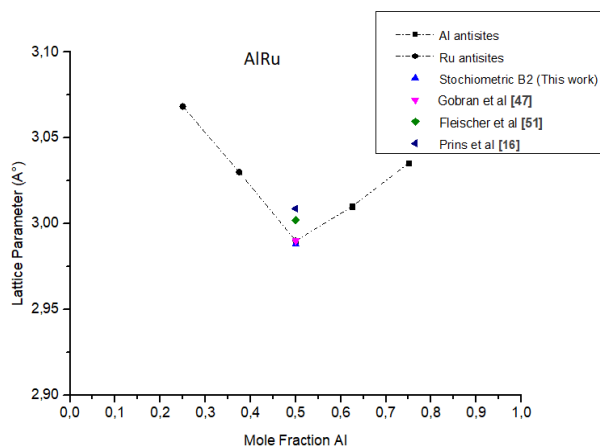


Fig. 7. Lattice parameter of B2 AlRu compared with available results.

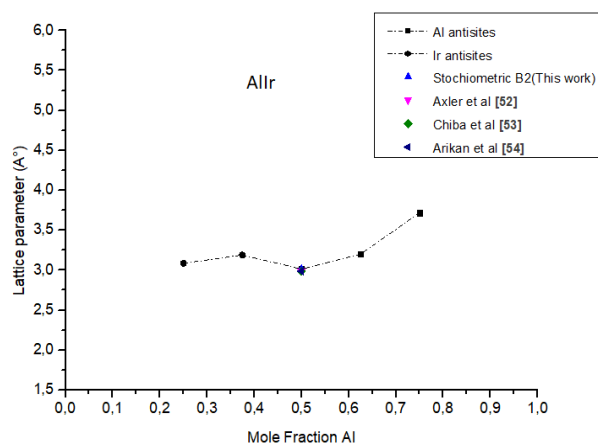


Fig. 8. Lattice parameter of B2 AlIr compared with available results.

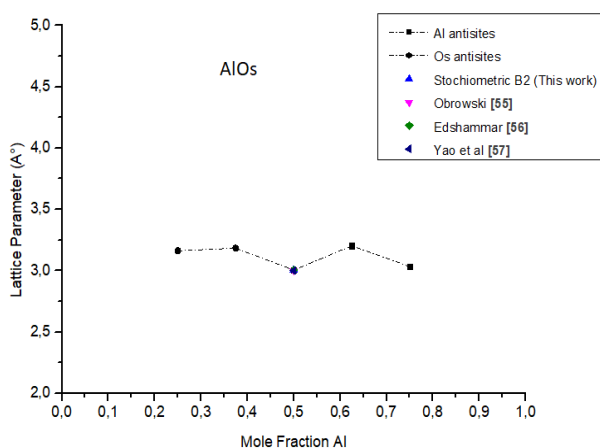


Fig. 9. Lattice parameter of B2 AlOs compared with available results.

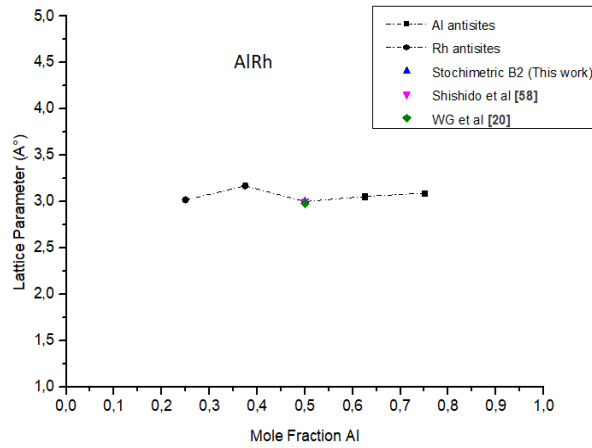


Fig. 10. Lattice parameter of B2 AlRh compared with available results.

Table I. Comparison of calculated formation enthalpies $\Delta_f H$ and lattice parameters (a) for AlRu, AlIr, AlOs, and AlRh in comparison with experimental and other theoretical results.

Phase		$\Delta_f H$ (eV/atom)	a (nm)
AlRu	Experiment	-0.649 [20]	0.2988 [47]
		-0.643 [48]	0.2992 [16]
		-0.644 [20]	0.2994 [59]
			0.303 [47]
			0.30079
	This work Other calculations	-0.639	0.30079
		-0.647 [48]	0.295 [62]
		-0.672 [20]	0.2967 [16]
		-0.604 [18]	0.30088 [16]
		-0.734 [60]	0.3005 [16]
	-0.603 [61]	0.3 [63]	
AlIr	Experiment	-0.963 [20]	0.29867 [52]
			0.2983 [64]
			0.2986 [53]
	This work Other calculations	-0.984	0.30125
		-0.953 [19]	0.3012 [19]
		-0.943 [20]	0.3020 [49]
		-0.969 [36]	0.3004 [49]
			0.3012 [19]
			0.302 [19]
			0.3028 [36]
	0.3 [63]		
AlOs	Experiment	-0.3995 [20]	
	This work	-0.3953	0.3025
	Other calculations		0.3005 [55] 0.3001 [49] 0.30166 [57]
AlRh	Experiment	-1.103 [20]	
	This work	-1.088	0.3001
	Other calculations	-1.097 [65]	0.298 [65]

The calculated formation enthalpies and lattice parameters for AlRu and AlIr show good agreement with both experimental and other theoretical values. For AlOs and AlRh, although there is limited directly comparable data available, the available results agree well with our calculations.

The results for AlRu agree well with other reported data, confirming that both Al antisites and Ruantisites are stable point defects. For AlIr, while there is limited directly comparable data, the available results agree well with ours, suggesting that both Al antisites and Irantisites are stable point defects. As for AlOs and AlRh, no directly comparable data are available, but the calculated enthalpies of formation indicate that both Al antisites and the corresponding TM antisites (TM = Os, Rh) have the lowest enthalpies, thus suggesting that AlOs and AlRh exhibit Al antisite and Rh antisite defects as their stable point defects, respectively.

Table2. The calculated formation enthalpies of isolated point defects for AlRu, AlIr, AlOs, and AlRh at $T=0K$.

Defect H_d (eV/defect)	
AlRu	
Al antisites Al_{Ru}	1.7300.068 [17]
Al vacancies Va_{Al}	5.3763.622 [17]
Ruantisites Ru_{Al}	4.0432.123 [17]
Ru vacancies Va_{Ru}	4.0680.912 [17]
AlIr	
Al antisites Al_{Ir}	1.145
Al vacancies Va_{Al}	2.952.570 [66]
Irantisites Ir_{Al}	2.92 2.567 [66]
Ir vacancies Va_{Ir}	2.795
AlOs	
Al antisites Al_{Os}	2.76
Al vacancies Va_{Al}	5.65
Osantisites Os_{Al}	4.92
Os vacancies Va_{Os}	3.69
AlRh	
Al antisites Al_{Rh}	1.20
Al vacancies Va_{Al}	1.93
Rh antisites Rh_{Al}	1.39
Rh vacancies Va_{Rh}	2.45

Table3. Formation enthalpies of complex defects in stoichiometric B2 AlTM (TM=Ru, Ir, Os and Rh) at $T = 0 K$.

Defect	H_d (eV/Defect)
AlRu	
Triple Ru ($0 \rightarrow 2 Va_{Ru} + Ru_{Al}$)	12.1794.338 [16]
Schottky ($0 \rightarrow Va_{Ru} + Va_{Al}$)	9.444 4.662 [16]
Exchange ($0 \rightarrow Ru_{Al} + Al_{Ru}$)	5.7733.462 [16]
Triple Al ($0 \rightarrow 2Va_{Al} + Al_{Ru}$)	12.482 8.447 [16]
Interbranche Ru ($Ru_{Al} \rightarrow 2Va_{Al}$)	6.709
Interbranche Al ($Al_{Ru} \rightarrow 2Va_{Ru}$)	6.406
AlIr	
Triple Ir ($0 \rightarrow 2 Va_{Ir} + Ir_{Al}$)	8.51
Schottky ($0 \rightarrow Va_{Ir} + Va_{Al}$)	5.745
Exchange ($0 \rightarrow Ir_{Al} + Al_{Ir}$)	4.065
Triple Al ($0 \rightarrow 2Va_{Al} + Al_{Ir}$)	7.045
Interbranche Ir ($Ir_{Al} \rightarrow 2Va_{Al}$)	2.98
Interbranche Al ($Al_{Ir} \rightarrow 2Va_{Ir}$)	4.445
AlOs	
Triple Os ($0 \rightarrow 2 Va_{Os} + Os_{Al}$)	12.3

Defect	H_d (eV/Defect)
Schottky ($0 \rightarrow Va_{Os} + Va_{Al}$)	9.34
Exchange ($0 \rightarrow Os_{Al} + Al_{Os}$)	7.68
Triple Al ($0 \rightarrow 2Va_{Al} + Al_{Os}$)	14.06
Interbranche Os ($Os_{Al} \rightarrow 2Va_{Al}$)	6.38
Interbranche Al ($Al_{Os} \rightarrow 2Va_{Os}$)	4.62
AIRh	
Triple Rh ($0 \rightarrow 2Va_{Rh} + Rh_{Al}$)	6.29
Schottky ($0 \rightarrow Va_{Rh} + Va_{Al}$)	4.38
Exchange ($0 \rightarrow Rh_{Al} + Al_{Rh}$)	2.59
Triple Co ($0 \rightarrow 2Va_{Al} + Al_{Rh}$)	5.06
Interbranche Rh ($Rh_{Al} \rightarrow 2Va_{Al}$)	2.47
Interbranche Al ($Al_{Rh} \rightarrow 2Va_{Rh}$)	3.70

The formation enthalpies several types of complex point defects at $T = 0$ K are given in Table 3 for B2 AlTM. As shown, the complex defects in the ground state are of exchange type in AlRu, one Ru antisite is replaced by one Al antisite. It can be observed that complex defects in AlOs are of interbranche Al type, which means that the occurrence of one Al antisite is matched by the disappearance of two Os vacancies. As can be seen in Table 3 also, the interbranche Ir and Rh defects have lower formation enthalpies than the other defects in AlIr and AlRh respectively, where two Ir and Rh vacancies appearance is associated with one Ir and Rh antisites respectively. The difference between our results and the available data for AlRu due to the calculations methods used to obtain the results of this work and those of [16] which are the SQS and the supercell approaches respectively.

3.3. Structures of defects at different temperatures

Fig. 11, 12, 13 and 14 illustrate the thermal defect concentrations calculated using the SQS approach in B2 AlTM (TM = Ru, Ir, Os, and Rh) at temperatures $T=2133$ K, $T=2293$ K, $T=1673$ K, and $T=1773$ K, respectively. The concentrations of these thermal defects are determined by applying the Wagner-Schottky model, utilizing the enthalpies of defect formation listed in Table 2. The results are then plotted as a function of the Aluminum composition.

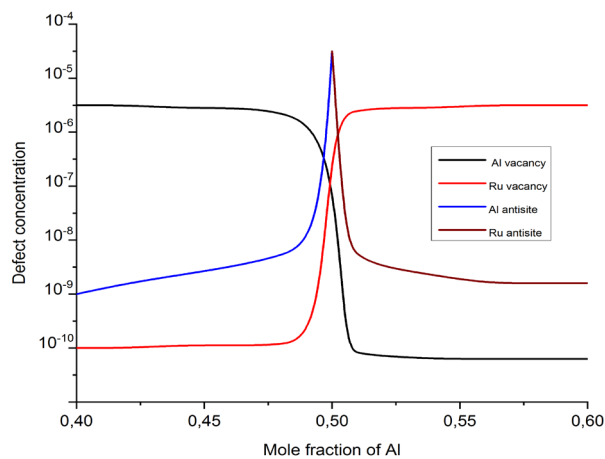


Fig. 11. Equilibrium thermal defects concentrations in B2 AlRu at $T=2133$ K.

In Fig. 11, For the Al-rich region of AlRu, the primary defects are Ru vacancy atoms. Conversely, in the Ru-rich region of AlRu, the predominant defects are Al vacancies, with each unit of Al vacancies corresponding to one unit of Ru vacancies. These vacancies constitute the Schottky-type defect. The defect structures in Al-rich side are of triple Ru-type, where

$2x(Va_{Ru}) \approx x(Ru_{Al})$ also the concentration of Ru antisites decreases with the increasing of Ru vacancies concentration. In Ru-rich side, the defects also are of triple Al-type where $2x(Va_{Al}) \approx x(Al_{Ru})$, where the Al antisites concentration increases with the decreasing of Al vacancies concentration. There is a complete absence of Al antisites and Ru antisites in Al-rich side and Ru-rich side respectively, their elevated concentrations form a peak at $x=0.5$ and decrease rapidly with deviation from stoichiometry.

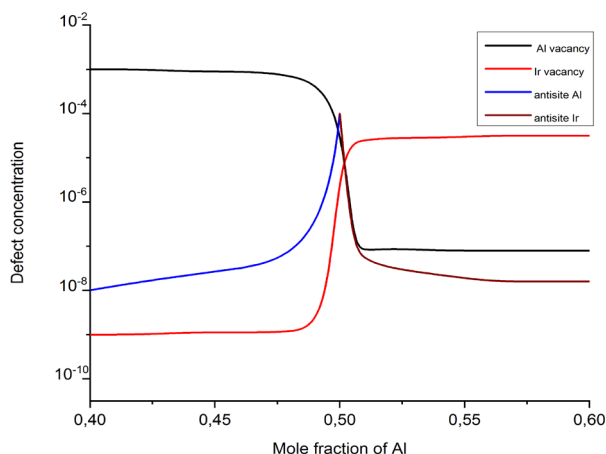


Fig. 12 Equilibrium thermal defects concentrations in B2 AlIr at $T=2293$ K.

In Fig.12, for the Al-rich region the primary thermal defects observed are Ir vacancies, while in the Ir-rich region they are Al vacancies, both representing Schottky defects. Additionally, in the Ir-rich region, the thermal defect structures include triple Al-type configurations, where approximately twice the concentration of Ir vacancies $2x(Va_{Ir}) \approx x(Ir_{Al})$, it is equivalent to the concentration of Ir atoms replacing Al atoms. Here, the concentration of Al antisites decreases with an increase in the concentration of Al vacancies. On the other side, in the Al-rich side, the defects are of Schottky-type. The peak observed at $x=0.5$ represents high concentrations of Irantisites and Al antisites, which decrease with deviation from stoichiometry.

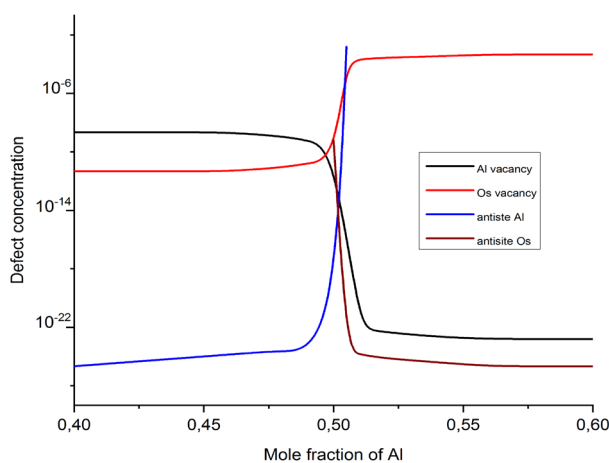


Fig.13. Equilibrium thermal defects concentrations in B2 AlOs at $T=1673$ K.

In Fig.13, The main thermal defects observed are Os vacancies in the Al-rich region and Al vacancies in the Os-rich region, both classified as Schottky defects. In this specific case, one

unit of Al vacancies is equivalent to one unit of Os vacancies. Schottky-type defects characterize the thermal defect structures observed in both the Al-rich and Os-rich sides. The peak observed at $x=0.5$ corresponds to a high percentage of Osantisites and Al antisites concentrations, which exist only in the Al-rich side and Ir-rich side, respectively. These concentrations decrease as we move away from stoichiometry.

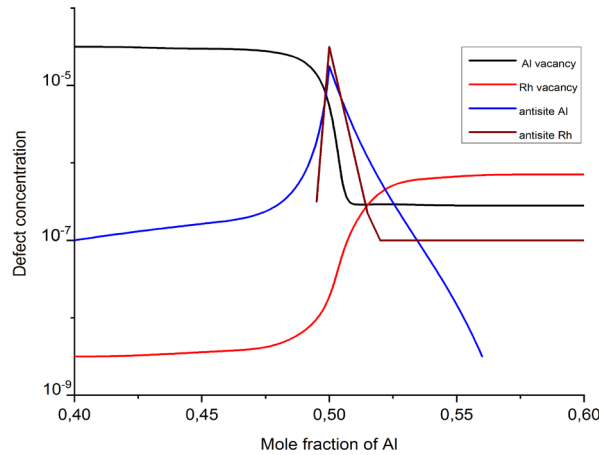


Fig.14. Equilibrium thermal defects concentrations in B2 AlRh at $T=1773$ K.

In Fig.14, The main thermal defects observed are Rh vacancies in the Al-rich region and Al vacancies in the Rh-rich region, consistent with the findings reported by Medasani et al.[67]. The exchange of vacancies between Al and Rh corresponds to a Schottky-type defect. In both the Al-rich and Rh-rich sides, the defect structures consist of triple Al-type and triple Rh-type, respectively, where approximately twice the concentration of Rh vacancies $2x(Va_{Rh})$ is equivalent to the concentration of Rh atoms replacing Al atoms $x(Al_{Rh})$, and similarly for Al vacancies. Here, the concentration of Al antisites and Rh antisites decreases with an increase in the concentration of Al vacancies and Rh vacancies in the Al-rich region and Rh-rich region, respectively. Additionally, the concentrations of Rh antisites and Al antisites, which appear only in the Al-rich region and Rh-rich region, respectively, pass through a peak at $x=0.5$ and decrease as we move away from stoichiometry.

Indeed, Fig.11,12,13 and 14 indicate that the major thermal defects in B2 AlTM are the Al vacancies and TM vacancies in the Al-rich side and TM-rich side, respectively, which constitute the Schottky defect. This is characterized by the reaction $x(Va_{Al})=x(Va_{TM})$, where one unit of Al vacancies is exchanged by one unit of TM vacancies. However, the values of Al and TM vacancies concentrations plotted in Fig. 14 do not achieve equality as defined in this reaction. Specifically, $(Va_{(Ru,Os)}) < x(Va_{Al})$ and $x(Va_{(Ir,Rh)}) > x(Va_{Al})$. This discrepancy may be attributed to the behavior of Al antisites and TM antisites. Interestingly, their concentrations peak at the stoichiometric composition. Consequently, the predominance of Al and TM antisites concentrations at the stoichiometric composition leads to the formation of a peak at this point ($x=0.5$), which impacts the concentrations of Al and TM vacancies. Another possible reason for this discrepancy could be the complete absence of Al antisites and TM antisites in the Al-rich region and TM-rich region, respectively, compared to their existence. This disrupted behavior, combined with the factors mentioned previously, contributes to obtaining these results in the study of thermal defects for the AlTM (TM = Ru, Ir, Os, and Rh) alloys.

4. Conclusion

In this study, the defect types and structure of stoichiometric binary B2 Aluminium-based crystalline compounds of transition metal, particularly platinum-group metals are presented. The formation enthalpies of isolated point defects in AlTM alloys across various concentrations using the (SQS) approach have been calculated. The Al-antisites are the major point defects in the Al-rich region, while the TM-antisites are the stable point defects along the TM-rich side. At finite temperature, the predominant thermal defects found using Wagner-Schottky model in the studied alloys are of Schottky-type. Overall, it can be concluded that the elements belonging to the same family (transition metals) or the same subfamily (platinum-group metals) and forming compounds based on the same element have the same behavior and show the same type of stable point defects at $T = 0$ K and finite temperature. The discrepancy between the results from the present study and some previous studies is due to the formation of antisites and vacancies, which are not taken into consideration in those studies. However, despite this discrepancy, our results remain close to the results from the literature.

References

- [1] H. G. Tang, X. F. Ma, W. Zhao, X. W. Yan and R. J. Hong, *Journal of Alloys and Compounds* 347, 228 (2002); [https://doi.org/10.1016/S0925-8388\(02\)00760-0](https://doi.org/10.1016/S0925-8388(02)00760-0)
- [2] M. Nobuki, D. Vanderschueren, and M. Nakamura, *Actametallurgica et materialia*42, 2623 (1994); [https://doi.org/10.1016/0956-7151\(94\)90204-6](https://doi.org/10.1016/0956-7151(94)90204-6)
- [3] M. A. Guitar, E.R. Moore and F. Mucklich, *Journal of Alloys and Compounds* 594, 165 (2014); <https://doi.org/10.1016/j.jallcom.2014.01.137>
- [4] M.A. Guitar and F. Mucklich, *Oxidation of Metals* 80, 423 (2013); <https://doi.org/10.1007/s11085-013-9409-8>
- [5] A. R. S. Bidabadi, M. H. Enayati, E. Dastanpoor, R. A. Varin and M. Biglari, *J Alloy Compd*, vol. 581, pp. 91-100, (2013); <https://doi.org/10.1016/j.jallcom.2013.07.037>
- [6] B. Grushko, J. Gwozdz and M. Yurechko, *Journal of Alloys and Compounds* 305, 219 (2000); [https://doi.org/10.1016/S0925-8388\(00\)00754-4](https://doi.org/10.1016/S0925-8388(00)00754-4)
- [7] L. M. Pike, Y. A. Chang and C. T. Liu, *ActaMaterialia*45, 3709 (1997); [https://doi.org/10.1016/S1359-6454\(97\)00028-1](https://doi.org/10.1016/S1359-6454(97)00028-1)
- [8] N. Acharya, B. Fatima, S. S. Chouhan and S. P. Sanyal, *Advanced Materials Research* 1047, 71 (2014); <https://doi:10.4028/www.scientific.net/AMR.1047.71>
- [9] H. L. Tuller and S. R. Bishop, *Annual Review of Materials Research* 41, 369 (2011); <https://doi.org/10.1146/annurev-matsci-062910-100442>
- [10] P. A. Varotsos, N. V. Sarlis and E. S. Skordas, *Crystals*12, 686 (2022); <https://doi.org/10.3390/cryst12050686>
- [11] C. Jiang, L.Q. Chen and Z.K. Liu, *ActaMaterialia*53, 2643 (2005); <https://doi.org/10.1016/j.actamat.2005.02.026>
- [12] M. Kogachi, and T. Haraguchi, *Materials Science and Engineering: A*312, 189 (2001); [https://doi.org/10.1016/S0921-5093\(00\)01892-X](https://doi.org/10.1016/S0921-5093(00)01892-X)
- [13] A. Kerboub, E. Belbacha, A. Hidoussi, Y. Djaballah and A. B. Bouzida, *Journal of Phase Equilibria and Diffusion*38, 143 (2017); <https://doi.org/10.1007/s11669-017-0526-y>
- [14] Y. A. Chang, and J. P. Neumann, *Progress in Solid State Chemistry*14, 221 (1982); [https://doi.org/10.1016/0079-6786\(82\)90004-8](https://doi.org/10.1016/0079-6786(82)90004-8)
- [15] J. Rogal, S. Divinski, M. W. Finnis, A. Glensk, J. Neugebauer, J. H. Perepezko, S. Schuwalow, M. H. F. Sluiter and B. Sundman, *Phys Status Solidi B* 251,97 (2014); <https://doi.org/10.1002/pssb.201350155>
- [16] S. Prins, R. Arroyave and Z. K. Liu, *ActaMaterialia*55, 4781 (2007); <https://doi.org/10.1016/j.actamat.2007.04.048>
- [17] R. Sot, M. Gokieli, H. Garbacz and K. J. Kurzydowski, *InżynieriaMateriałowa* 28,463 (2007).

- [18] H. T. Stokes, L. L. Boyer and M. J. Mehl, *Physical Review B* 54, 7729 (1996); <https://doi.org/10.1103/PhysRevB.54.7729>
- [19] W. Jung and O.J. Kleppa, *The Journal of Chemical Thermodynamics* 23, 147 (1991); [https://doi.org/10.1016/S0021-9614\(05\)80291-5](https://doi.org/10.1016/S0021-9614(05)80291-5)
- [20] W. J. WG and O.J. Kleppa, *Metallurgical and Materials Transactions A* 23, 53 (1992); <https://doi.org/10.1007/BF02654036>
- [21] M. Wei, A. C. Huang, C. M. Shu, et L. Zhang, *Sci. Rep.* 9, 1592 (2019); <https://doi.org/10.1038/s41598-018-38434-1>
- [22] C. Colinet and J. C. Tedenac, *CALPHAD* 54, 16 (2016); <https://doi.org/10.1016/j.calphad.2016.05.001>
- [23] A. Zunger, S. H. Wei, L. G. Ferreira, and J. E. Bernard, *Phys. Rev. Lett* 65, 363 (1990); <https://doi.org/10.1103/PhysRevLett.65.353>
- [24] S. Wei, L.G. Ferreira, J.E. Bernard and A. Zunger, *Phys. Rev. B* 42, 9622 (1990); <https://doi.org/10.1103/PhysRevB.42.9622>
- [25] E. F. Larsen, *Comput. Mater. Sci* 98, 220 (2015); <https://doi.org/10.1016/j.commatsci.2014.11.018>
- [26] C. Jiang, C. Wolv, J. Sofo, L.Q. Chen, and Z. K. Liu, *Phys. Rev B* 69, 214202 (2004); <https://doi.org/10.1103/PhysRevB.69.214202>
- [27] C. Wolverton, *Acta Materialia* 49, 3129 (2001); [https://doi.org/10.1016/S1359-6454\(01\)00229-4](https://doi.org/10.1016/S1359-6454(01)00229-4)
- [28] Y. P. Xie, and S. J. Zhao, *Computational Materials Science* 50, 2586 (2011); <https://doi.org/10.1016/j.commatsci.2011.03.046>
- [29] J. V. Pezold, A. Dick and M. Friák, *Phys. Rev. B* 81, 94 (2010).
- [30] Z. Wen, Y. Zhao, J. Tian, S. Wang, Q. Guo and H. Hou, *J. Mater. Sci* 54, 2566 (2019); <https://doi.org/10.1007/s10853-018-2943-7>
- [31] S. H. Wei, and A. Zunger, *Phys. Rev. Lett* 76, 664 (1996); <https://doi.org/10.1103/PhysRevLett.76.664>
- [32] P. Soderlind and B. Sadigh, *Phys. Rev. Lett* 92, 185702 (2004). <https://doi.org/10.1103/PhysRevLett.92.185702>
- [33] F. Tasnadi, B. Alling, C. Hoglund, G. Wingqvist, J. Birch, L. Hultman, and I. A. Abrikosov, *Phys. Rev. Lett* 104, 137601 (2010). <https://doi.org/10.1103/PhysRevLett.104.137601>
- [34] P. A. Korzhavyi, A. V. Ruban, A. Y. Lozovoi, Yu. Kh. Vekilov, I. A. Abrikosov and B. Johansson, *Physical Review B* 61, 6003 (2000); <https://doi.org/10.1103/PhysRevB.61.6003>
- [35] C. Fu and J. Zou, *Acta Materialia* 44, 1471 (1996); [https://doi.org/10.1016/1359-6454\(95\)00297-9](https://doi.org/10.1016/1359-6454(95)00297-9)
- [36] Y. Song, Z. Guo, R. Yang and D. Li, *Acta Materialia* 49, 1647 (2001); [https://doi.org/10.1016/S1359-6454\(01\)00052-0](https://doi.org/10.1016/S1359-6454(01)00052-0)
- [37] J. Nyman, G. M. Day, *CrystEngComm* 17, 5154 (2015); <https://doi.org/10.1039/C5CE00045A>
- [38] K. Parlinski, P. Jochym, R. Kozubski and P. Oramus, *Intermetallics* 11, 157 (2003); [https://doi.org/10.1016/S0966-9795\(02\)00195-4](https://doi.org/10.1016/S0966-9795(02)00195-4)
- [39] C. Jiang, L.Q. Chen and Z.K. Liu, *Intermetallics* 14, 248 (2006); <https://doi.org/10.1016/j.intermet.2005.05.012>
- [40] P. E. Blöchl, *Physical Review B* 50, 17953 (1994); <https://doi.org/10.1103/PhysRevB.50.17953>
- [41] G. Kresse, D. Joubert, *Physical Review B* 59, 1758 (1999); <https://doi.org/10.1103/PhysRevB.59.1758>
- [42] J. P. Perdew, K. Burke and M. Ernzerhof, *Phys Rev Lett* 77, 3865 (1996); <https://doi.org/10.1103/PhysRevLett.77.3865>
- [43] G. Kresse, M. Marsman and J. Furthmüller, *VASP the Guide*, University of Vienna (2012).
- [44] H. J. Monkhorst and J. D. Pack, *Physical Review B* 13, 5188 (1976); <https://doi.org/10.1103/PhysRevB.13.5188>
- [45] B. Yanchitsky and A. Timoshevskii, *Computer Physics Communications* 139, 235 (2001); [https://doi.org/10.1016/S0010-4655\(01\)00212-0](https://doi.org/10.1016/S0010-4655(01)00212-0)
- [46] R. R. Sot, R.J. Kurzydowski, *Mater Sci-Poland* 23, 407 (2005).

- [47] H. Gobran, K.W. Liu, D. Heger and F. Mucklich, *ScriptaMaterialia*49, 1097 (2003); <https://doi.org/10.1016/j.scriptamat.2003.08.005>
- [48] B. Wen, J. Zhao, F. Bai and T. Li, *Intermetallics*16, 333 (2008); <https://doi.org/10.1016/j.intermet.2007.11.003>
- [49] Y. Pan, M. Wen, L. Wang, X. Wang, Y.H. Lin and W.M. Guan, *Journal of Alloys and Compounds* 648, 771 (2015); <https://doi.org/10.1016/j.jallcom.2015.07.058>
- [50] T. Hu, Z. Ruan, T. Fan, D. Chen, Y. Wu and P. Tang, *Solid State Communications* 376, 115361 (2023); <https://doi.org/10.1016/j.ssc.2023.115361>
- [51] R. L. Fleischer, *Acta Metallurgica et Materialia*41, 863 (1993); [https://doi.org/10.1016/0956-7151\(93\)90020-S](https://doi.org/10.1016/0956-7151(93)90020-S)
- [52] K. Axler and R.B. Roof, *Adv. X-Ray Anal*29, 333 (1986); <https://doi.org/10.1154/S0376030800010429>
- [53] A. Chiba, T. Ono, X.G. Li and S. Takahashi, *Intermetallics*6, 35 (1998); [https://doi.org/10.1016/S0966-9795\(97\)00051-4](https://doi.org/10.1016/S0966-9795(97)00051-4)
- [54] N. Arikan, Z. Charifi, H. Baaziz, Ş. Uğur, H. Ünver and G. Uğur, *Journal of Physics and Chemistry of Solids*77, 126 (2015); <https://doi.org/10.1016/j.jpics.2014.10.007>
- [55] W. Obrowski, *Naturwissenschaften* 47, 14 (1960); <https://doi.org/10.1007/BF00628450>
- [56] L. Edshammar, *Acta Chem Scand*19, 871 (1965).
- [57] G. Yao, Y. Liu, W. Zhang, X. An, Y. Chen, H. Lei, Y. Fu, Z. Jiang, Y. Zhao, X. Wang, L. Cao and W. Wu, *Journal of Alloys and Compounds*581, 109 (2013); <https://doi.org/10.1016/j.jallcom.2013.07.053>
- [58] T. Shishido and H. Takei, *J. Less-Comm. Met*119, 75 (1986); [https://doi.org/10.1016/0022-5088\(86\)90197-9](https://doi.org/10.1016/0022-5088(86)90197-9)
- [59] A. Sabariz and G. Taylor, *MRS*460, 611 (1996); <https://doi.org/10.1557/PROC-460-611>
- [60] W. Lin, J. Xu and A. J. Freeman, *Journal of Materials Research* 7, 592 (1992); <https://doi.org/10.1557/JMR.1992.0592>
- [61] D. N. Manh and D. G. Pettifor, *Intermetallics*7, 10 (1999); [https://doi.org/10.1016/S0966-9795\(99\)00040-0](https://doi.org/10.1016/S0966-9795(99)00040-0)
- [62] L. E. Edshammar, *Acta Chemica Scandinavica* 20, 427 (1966).
- [63] B. Grushko, T. Velikanova, *Computer Coupling of Phase Diagrams and Thermochemistry* 31, 217 (2007); <https://doi.org/10.1016/j.calphad.2006.12.002>
- [64] H. Schulz, K. Ritapal, W. Bronger, W. Klemm and Z. Anorg, *Allgem. Chem*357, 299 (1968).
- [65] V. G. Khoruzhaya, K. E. Kornienko and P. S. Martsenyuk, *Powder Metallurgy and Metal Ceramics* 45, 251 (2006); <https://doi.org/10.1007/s11106-006-0072-3>
- [66] Y. Pan and M. Wen, The influence of vacancy on the mechanical properties of IrAlcoating: First-principles calculations, *Thin Solid Films*664, 46 (2018); <https://doi.org/10.1016/j.tsf.2018.08.028>
- [67] B. Medasani, A. Gamst, H. Ding, W. Chen, K. A. Persson, M. Asta and A. Canning, *npj Computational Materials* 2, 1 (2016); <https://doi.org/10.1038/s41524-016-0001-z>